

## Supporting Information

### **Enhanced Lithium-Ion Storage of SiO<sub>x</sub>@C Anode Enabled by Carbon Coating Coupling with MXene as a Conductive Binder**

Zhenqiang Liu,<sup>†a</sup> Yong Yang,<sup>†a</sup> Qizhen Zhu,<sup>\*a</sup> Meng Li,<sup>\*b</sup> and Bin Xu<sup>\*a,c</sup>

<sup>a</sup> State Key Laboratory of Organic-Inorganic Composites, Beijing Key Laboratory of Electrochemical Process and Technology for Materials, Beijing University of Chemical Technology, Beijing 100029, China.

<sup>b</sup> Research Institute of Chemical Defense, Academy of Military Sciences, Beijing 102205, China.

<sup>c</sup> Shaanxi Key Laboratory of Chemical Reaction Engineering, School of Chemistry and Chemical Engineering, Yan'an University, Yan'an 716000, China.

E-mail: xubin@mail.buct.edu.cn; zhuqz@mail.buct.edu.cn; limengfighting@163.com

<sup>†</sup> These two authors contributed equally to this work.

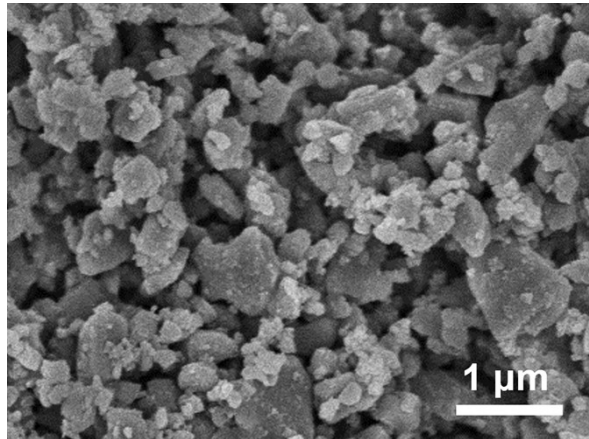


Fig. S1 SEM image of ball-milled  $\text{SiO}_x$ .

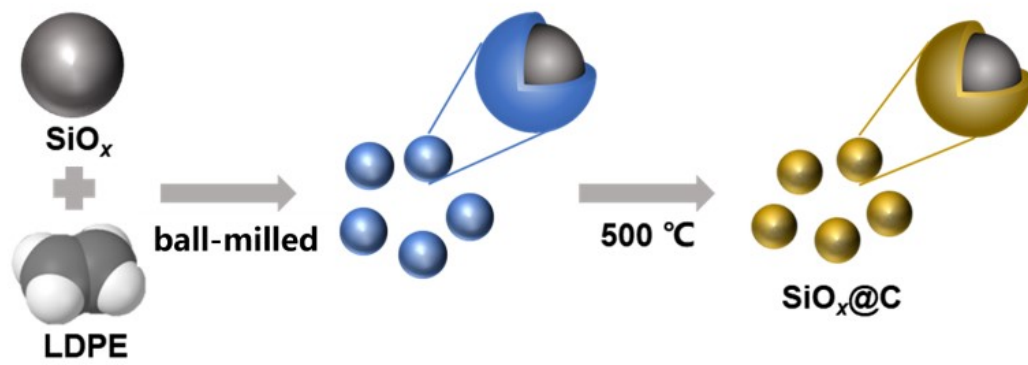
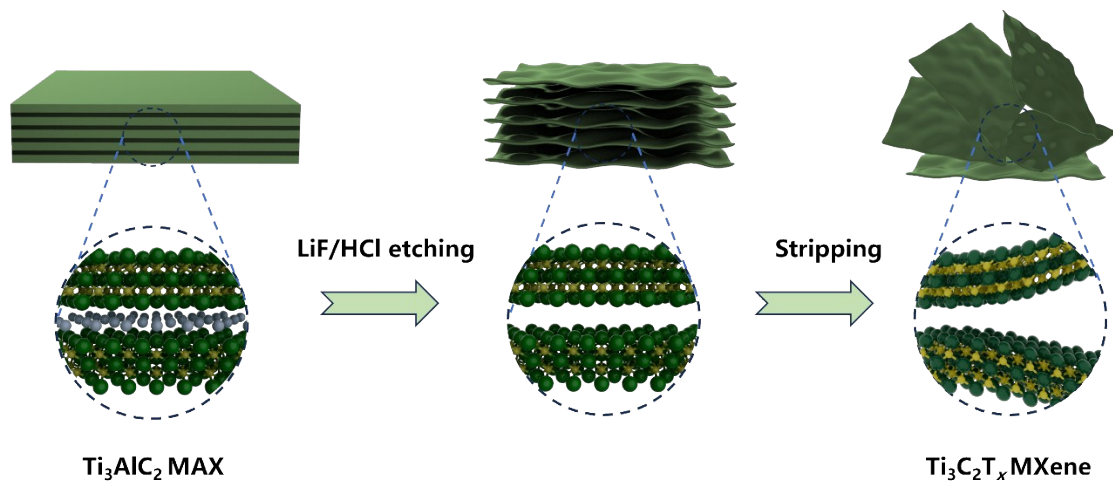
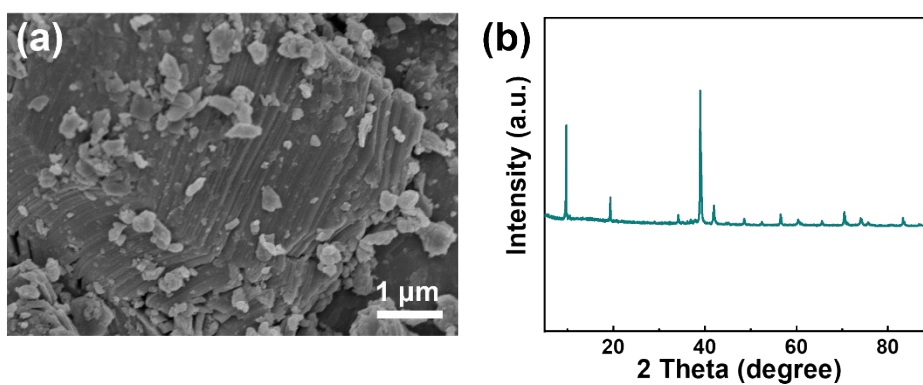


Fig. S2 Schematic for the preparation of  $\text{SiO}_x@C$ .



**Fig. S3** Schematic for the preparation of Ti<sub>3</sub>C<sub>2</sub>T<sub>x</sub> MXene.



**Fig. S4** (a) SEM image and (b) XRD pattern of Ti<sub>3</sub>AlC<sub>2</sub> powder.

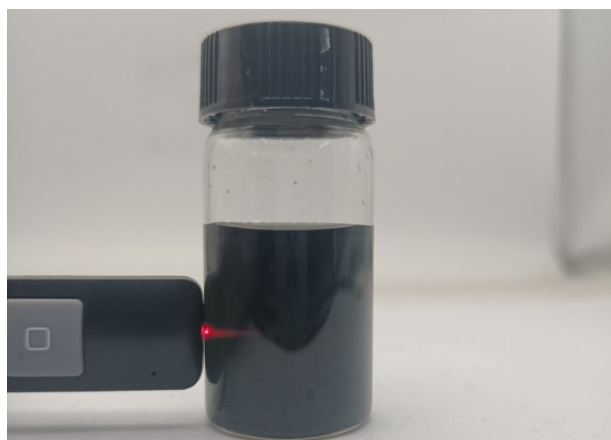


**Fig. S5** Optical image of  $\text{Ti}_3\text{C}_2\text{T}_x$  MXene dispersion.

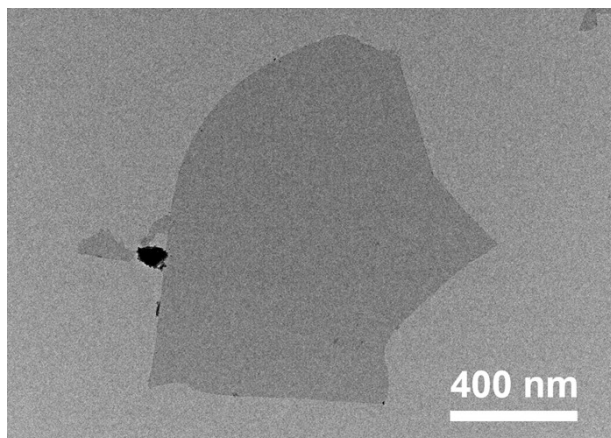


**Fig. S6** TEM image of  $\text{Ti}_3\text{C}_2\text{T}_x$  MXene.

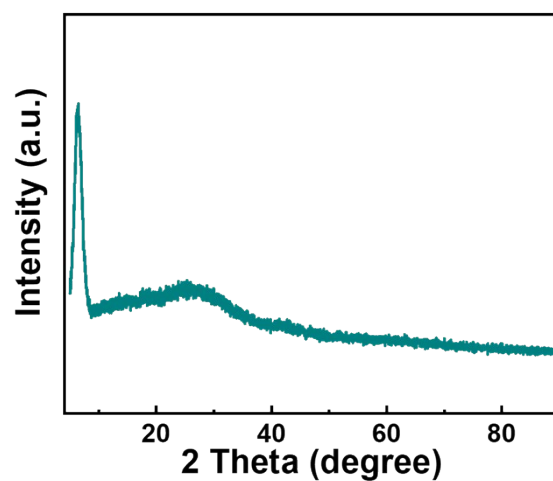


**Fig. S7** XRD pattern of  $\text{Ti}_3\text{C}_2\text{T}_x$  MXene.

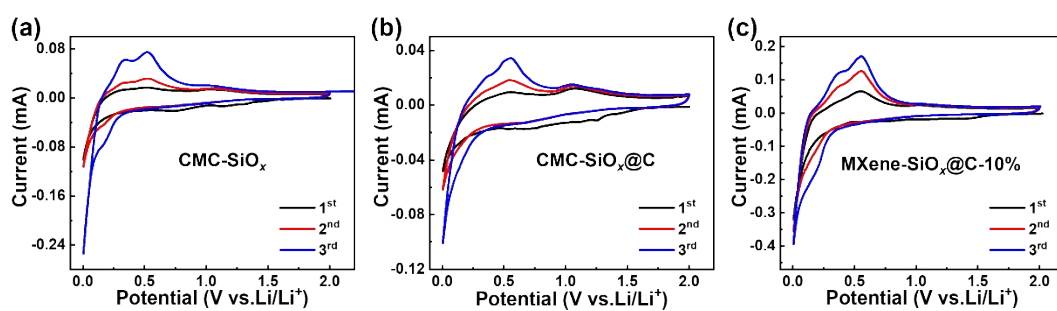


**Fig. S8** CV curves of (a)  $\text{CMC-SiO}_x$ , (b)  $\text{CMC-SiO}_x@\text{C}$  and (c)  $\text{MXene-SiO}_x@\text{C-10\%}$

at  $0.1 \text{ mV s}^{-1}$ .

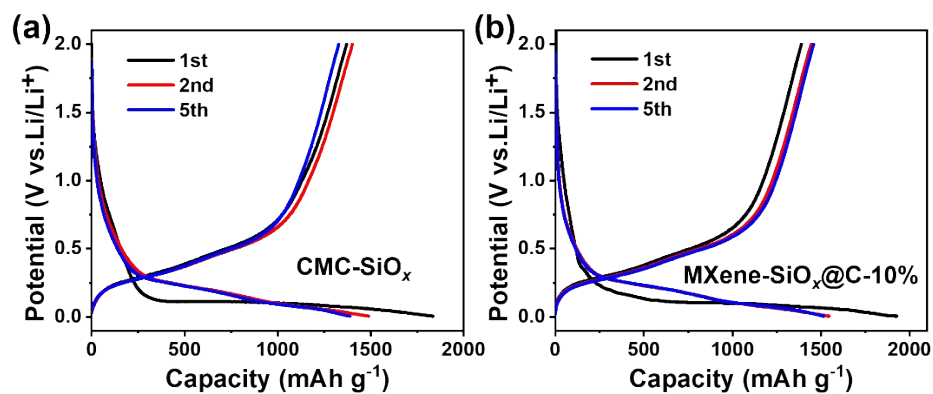


**Fig. S9** Charge/discharge curves of (a) CMC-SiO<sub>x</sub> and (b) MXene-SiO<sub>x</sub>@C-10% at 0.1 A g<sup>-1</sup>.

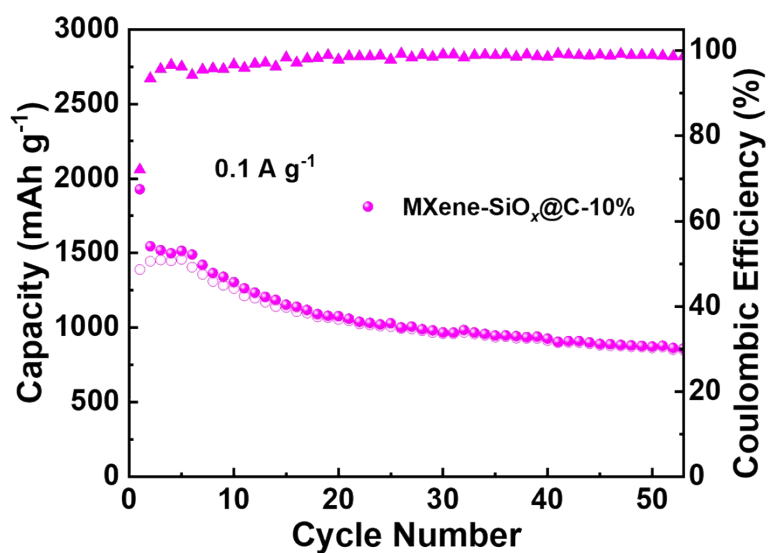


**Fig. S10** Cycling performance of MXene-SiO<sub>x</sub>@C-10%.

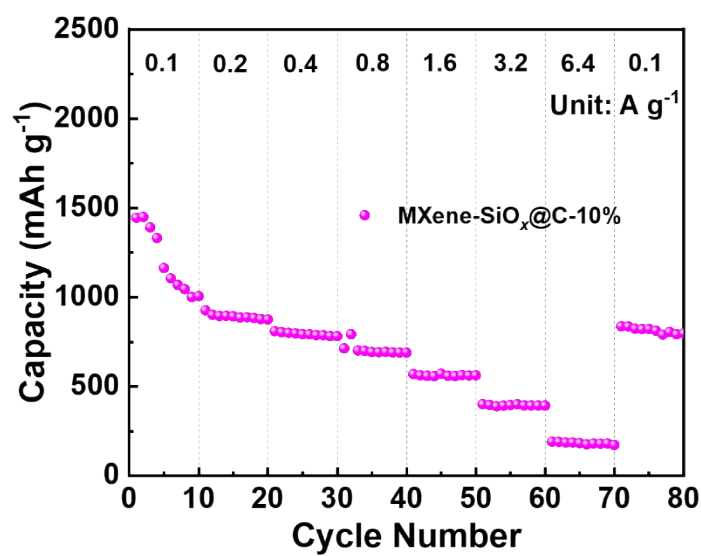


Fig. S11 Rate capability of MXene-SiO<sub>x</sub>@C-10%.

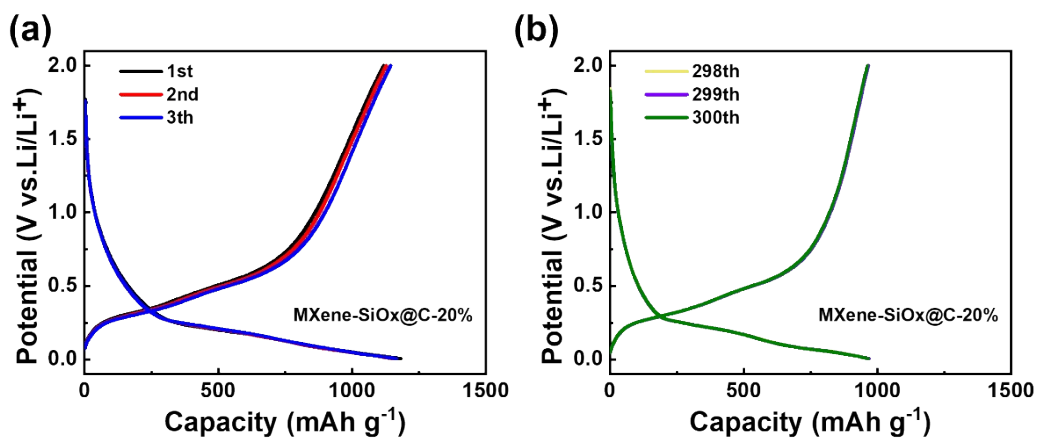
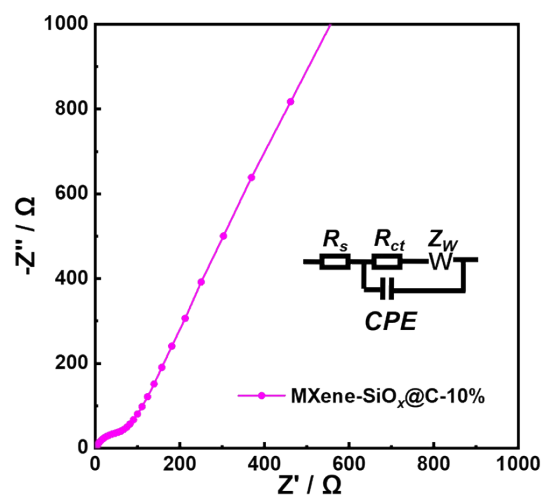
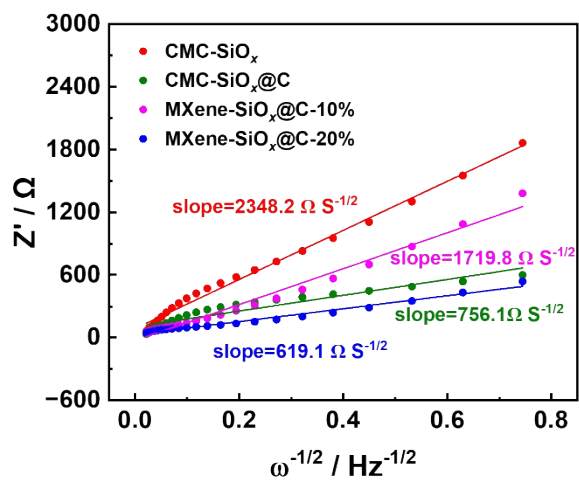


Fig. S12 Charge/discharge curves of MXene-SiO<sub>x</sub>@C-20% at (a) 1~3 and (b)

298~300 cycles at 0.8 A g<sup>-1</sup>.



**Fig. S13** Nyquist plots of MXene-SiO<sub>x</sub>@C-10% with the equivalent circuit in the inset.



**Fig. S14** Relationship between  $Z'$  and  $\omega^{-1/2}$  in the low-frequency region of EIS spectra of the electrodes.



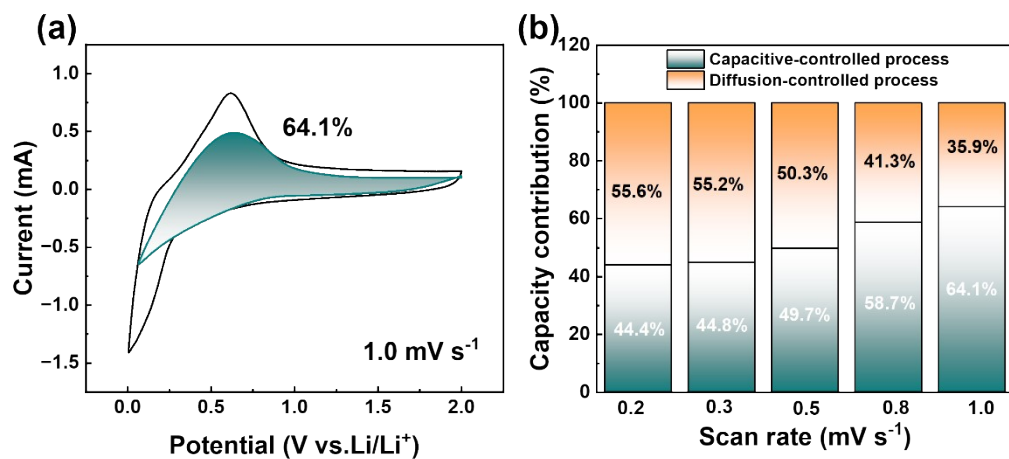


**Fig. S15** (a) Contribution ratio of the capacitive process of MXene-SiO<sub>x</sub>@C-20% at 1.0 mV s<sup>-1</sup>; (b) Capacitive contribution of MXene-SiO<sub>x</sub>@C-20% at different scanning rates in the range of 0.2~1 mV s<sup>-1</sup>.

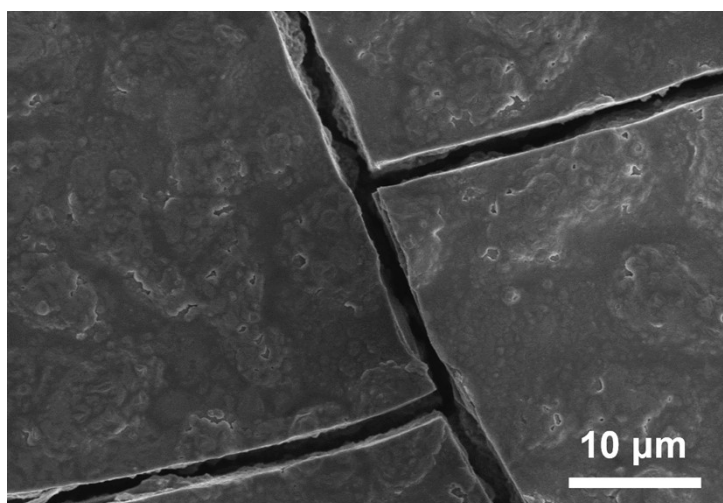


**Fig. S16** SEM image of MXene-SiO<sub>x</sub>@C-10% after 50 cycles at 0.1 A g<sup>-1</sup>.

**Table S1** EIS parameters of the electrodes.

	$R_s$ ( $\Omega$ )	$R_{ct}$ ( $\Omega$ )
CMC-SiO <sub>x</sub>	0.5	635.1
CMC-SiO <sub>x</sub> @C	1.7	214.0
MXene-SiO <sub>x</sub> @C-10%	1.9	82.7
MXene-SiO <sub>x</sub> @C-20%	2.2	41.9